Changes in the Apomyoglobin Folding Pathway Caused by Mutation of the Distal Histidine Residue[†]

Carlos Garcia, Chiaki Nishimura, Silvia Cavagnero,[‡] H. Jane Dyson,* and Peter E. Wright*

Department of Molecular Biology and Skaggs Institute for Chemical Biology, The Scripps Research Institute, 10550 North Torrey Pines Road, La Jolla, California 92037

Received May 4, 2000

ABSTRACT: Factors governing the folding pathways and the stability of apomyoglobin have been examined by replacing the distal histidine at position 64 with phenylalanine (H64F). Acid and urea-induced unfolding experiments using CD and fluorescence techniques reveal that the mutant H64F apoprotein is significantly more stable than wild-type apoMb. Kinetic refolding studies of this variant also show a significant difference from wild-type apoMb. The amplitude of the burst phase ellipticity in stopped-flow CD measurements is increased over that of wild-type, an indication that the secondary structure content of the earliest kinetic intermediate is greater in the mutant than in the wild-type protein. In addition, the overall rate of folding is markedly increased. Hydrogen exchange pulse labeling was used to establish the structure of the initial intermediate formed during the burst phase of the H64F mutant. NMR analysis of the samples obtained at different refolding times indicates that the burst phase intermediate contains a stabilized E helix as well as the A, G, and H helices previously found in the wild-type kinetic intermediate. Replacement of the polar distal histidine residue with a nonpolar residue of similar size and shape appears to stabilize the E helix in the early stages of folding due to improved hydrophobic packing. The presence of a hydrophilic histidine at position 64 thus exacts a price in the stability and folding efficiency of the apoprotein, but this residue is nevertheless highly conserved among myoglobins due to its importance in function.

The detailed mechanisms by which the primary sequence of a protein encodes its tertiary structure, and by which a protein spontaneously acquires its native fold, are still unclear. Apomyoglobin (apoMb)[1] provides an exceptionally versatile system to investigate the factors that govern the rate and mechanism of protein folding. At neutral pH, apoMb has a well-defined globular structure, comprising seven helical segments (A−E, G, H) packed to form a compact hydrophobic core (*1*, *2*): the F helix of holomyoglobin, which contributes a histidine ligand for binding the heme, is dynamically disordered in the apoprotein. As the pH is lowered, an equilibrium molten globule intermediate is formed near pH 4 which is characterized by a substantial α-helical content (about 35% compared to 55% in native apoMb) (*3*). Using NMR hydrogen exchange trapping experiments, Hughson et al. (*4*) showed that this compact intermediate contains helical structure in the A, G, and H regions. Kinetic studies of apoMb using stopped-flow and quench-flow techniques revealed the formation of a kinetic intermediate during the first 6 ms of the refolding process with a pattern of protection similar to the equilibrium intermediate at pH 4 (*5*). Subsequent kinetic studies strongly suggested that the intermediate was on-pathway (*6*), and quench-flow amide proton exchange combined with mass spectrometry confirmed that apomyoglobin folds by a single pathway and that the intermediate is obligatory (*7*).

Factors governing the overall stability and secondary structure of the apomyoglobin intermediate are still not well understood. Stability of individual regions could be crucial both to the overall stability and to the folding pathway of apoMb. Perturbation of folding and stability by the introduction of mutations at specific sites has been extensively used to explore folding pathways (*8*). Our approach is to select mutations to test hypotheses related to the folding of apoMb, and we have recently applied this approach in the elucidation of the role of the H helix in the earliest folding events (*9*). In the present work, we have investigated the effects on the folding pathway of a mutation that is known to stabilize the apoprotein (*10*).

Mutants of myoglobin where the distal histidine (His E7; His 64), located in the E helix, has been replaced by an apolar residue have been extensively characterized by Olson and co-workers (*11*−*13*). The His 64-Phe mutant in particular has been shown to have increased stability in the apo-form relative to wild-type (*10*). The highly conserved distal histidine is thought to play a functional role, at the expense of globin stability, by regulating O_2 affinity, inhibiting autoxidation, and discriminating against CO binding (*13*). Polar amino acids in the distal heme pocket can inhibit loss of heme by forming hydrogen bonds with coordinated water; however, following heme dissociation, such residues desta-

[†] This work was supported by Grants DK34909 (P.E.W.) and GM57374 (H.J.D.) from the National Institutes of Health and in part by the Wills Foundation (S.C.).

* To whom correspondence should be addressed.

[‡] Present address: Department of Chemistry, University of Wisconsin−Madison, 1101 University Ave., Madison, WI 53706.

[1] Abbreviations: NMR, nuclear magnetic resonance; CD, circular dichroism; apoMb, apomyoglobin; H64F, His64Phe mutant of apomyoglobin; pH*, measured pH of a D_2O solution, uncorrected for solvent isotope effect.

10.1021/bi0010266 CCC: $19.00
Published on Web 08/18/2000

bilize the native apomyoglobin structure by causing solvation of the heme pocket (*10*).

Both the native, folded form of apomyoglobin and the folding intermediate found at moderate concentrations of guanidine hydrochloride are stabilized in the H64F mutant relative to the wild-type protein (*10*). This suggested that the substitution of His by Phe could have an influence on the folding pathway of the protein as well as its stability. We have examined in detail the folding kinetics of the H64F mutant protein, and have found significant changes in the dominant folding pathway and in the structure of the molten globule intermediate.

MATERIALS AND METHODS

Protein Preparation. (A) Isolation and Purification of Wild-Type and H64F Mutant ApoMb. Wild-type recombinant sperm whale apomyoglobin was expressed in *Escherichia coli* and purified using previously described methods (*14*). Construction of the H64F mutant gene was carried out by polymerase chain reaction (PCR). The final PCR product containing the complete sequence of the H64F apoMb was cleaved with specific restriction enzymes (*Nde*I and *Kpn*I), gel purified, and ligated into a pET17b vector (Novagen). The vector harboring the mutant gene was first transformed into *E. coli* XL1-blue to duplicate the gene for sequencing, and then into BL21(DE3) (pLysS) strain (Stratagene) for expression.

Unlabeled samples of both wild-type and H64F apoMb were prepared from *E. coli* grown in LB media. ^{15}N- and ^{13}C-labeled protein for NMR was prepared using minimal medium according to published methods (*14*). Cultures were grown at 37 °C and induced at $A_{600} = 1.0$ with isopropyl-thiogalactose (IPTG). After at least 5 h, the cells were harvested by centrifugation and lysed using lysozyme. The inclusion bodies were dissolved in 100% acetonitrile/0.1% trifluoroacetic acid (TFA) using sonication. The resulting solution of the apoprotein was diluted 3-fold in HPLC Buffer A (0.1% TFA/water) and purified by reverse-phase HPLC using a 100% acetonitrile gradient solution containing 0.1% TFA as mobile phase. The lyophilized protein was checked for purity by SDS gel electrophoresis and mass spectrometry.

(B) Heme Reconstitution. The wild-type and H64F mutant holoproteins were reconstituted as follows. The lyophilized apoprotein was denatured in 0.5 mL of sodium acetate buffer (10 mM, pH 6.0) containing 6 M urea at 4 °C. Refolding was achieved by rapid 10-fold dilution of the urea-denatured protein into sodium acetate buffer (10 mM, pH 6.0), also at 4 °C. Under these conditions, the protein refolds very rapidly. Bovine hemin (Sigma) was dissolved in 10 mM sodium hydroxide and added to 25 mL of phosphate buffer (50 mM, pH 8.0) containing 100 mM KCN. This solution was immediately added in a 1.2-fold molar excess to the refolded apoprotein solution, with stirring at 4 °C. The solution of reconstituted holoprotein was concentrated with an Amicon (YM10 membrane) concentrator and exchanged with 50 mM phosphate buffer without KCN. Under these conditions, the free heme precipitated on the membrane.

(C) Samples for NMR. NMR measurements were performed on the carbon monoxide complex, which was prepared by reduction of CO-saturated protein solution with 10-fold molar excess of freshly prepared sodium dithionite dissolved in 10 mM sodium hydroxide saturated with CO. The excess reductant was removed by passing the protein solution through a PD-10 column equilibrated with CO-saturated phosphate buffer (50 mM, pH 5.8) in 95% H_2O/5% D_2O. The sample was directly collected in an NMR tube under CO. To obtain a single heme isomer, the sample was incubated at 35 °C for 12 h prior to NMR analysis (*5*).

Spectroscopy. (A) Circular Dichroism. Far-UV circular dichroism (CD) spectra were measured to determine the helical content of both wild-type and H64F apoMb. CD data were collected on an Aviv 60DS spectropolarimeter equipped with a temperature-controlled cell holder, using 1 cm cuvettes at room temperature. Spectra were recorded from 190 to 260 nm and were an average of two scans with a time constant of 1 s and a step size of 1 nm. Both proteins were dissolved in 10 mM sodium acetate buffer at pH 6.0, and their concentrations were carefully verified by amino acid analysis and by UV absorbance at 280 nm (extinction coefficient of 15 900 $M^{-1}cm^{-1}$).

(B) Fluorescence. Fluorescence measurements were performed on an SLM MC 200 spectrofluorometer, using a 1 cm path length. Excitation was at 278 nm, and fluorescence emission was monitored at 320 nm. Excitation and emission bandwidths were set to 4 nm. Steady-state fluorescence anisotropy was recorded at 320 nm. Data were averaged over 10 measurements. All measurements were done at room temperature, and the concentration used for both wild-type and H64F mutant apomyoglobins was 3 μM.

(C) Nuclear Magnetic Resonance. All NMR experiments were performed at 35 °C on a Bruker AMX500 spectrometer equipped with gradients. ^{15}N-^{1}H HSQC (*15*) experiments were recorded with ^{1}H and ^{15}N spectral widths of 5000 and 1667 Hz, respectively. The ^{1}H carrier was placed at the H_2O frequency during the pulse train and shifted to the center of the amide protons during the acquisition, while the ^{15}N carrier was placed at 120 ppm. Data were acquired in the indirect dimension using the TPPI-States method (*16*).

Constant-time HNCA (*17*) and CBCA(CO)NH (*18*) spectra were recorded for resonance assignment of the H64F mutant. For the HNCA experiment, the ^{13}C carrier was placed at 53.8 ppm. ^{13}CO pulses were generated at 177 ppm. The $^{13}C\alpha$ spectral width was 3111 Hz. A total of 1024, 27, and 32 complex points were acquired in the ^{1}H, ^{15}N, and ^{13}C dimensions, respectively. The constant-time CBCA(CO)NH experiment was recorded with the ^{13}C carrier placed at 40.0 ppm, and the $^{13}C\alpha\beta$ spectral width was 7280 Hz. A total of 1024, 29, and 47 complex points were acquired in the ^{1}H, ^{15}N, and ^{13}C dimensions, respectively.

The NMR spectra were processed and analyzed on a Silicon Graphics computer using Felix 97 (Molecular Simulations Inc.) or NMRView (*19*).

Kinetic Refolding Measurements. The kinetics of refolding of wild-type and H64F mutant apoMb were measured at 4 °C on an Applied Photophysics DX-17M stopped-flow instrument, using both CD detection and fluorescence emission of the intrinsic tryptophan residues. Only the CD-detected experiments are reported here; the fluorescence measurements gave identical results. The protein was unfolded in 10 mM sodium acetate buffer and 6 M urea at pH 6.0. Refolding experiments were carried out by rapid 1 to 6 dilution of the urea/protein solution in 10 mM sodium acetate buffer at pH 6.0, giving a final urea concentration of 1 M.

The protein concentration was 10 μM, and the kinetic traces were averaged over 10 measurements.

Quench-Flow Hydrogen−Deuterium Exchange. Hydrogen exchange pulse labeling of wild-type and H64F mutant apoMb was performed at 5 °C using standard methods (*20*, *21*) in a Biologic model QFM-5 rapid mixing quench-flow apparatus. The protein (about 2.5 mg/mL) was unfolded in sodium acetate buffer (10 mM, pH 5.9) in H_2O solution containing 6 M urea. Refolding was initiated by a rapid 8.5-fold dilution into 10 mM sodium acetate buffer at pH* 5.9 in D_2O for variable time periods (6 ms, 37 ms, 74 ms, 105 ms, 200 ms, 300 ms, 500 ms, 1 s, 2 s, 4 s, 6 s). Pulse labeling was carried out using CAPS buffer in D_2O to increase the pH* to 10.1 to exchange unprotected amide protons. After 20 ms, the pH* was rapidly decreased to 6.0 by dilution with quench buffer (300 mM MOPS, pH* 1.6). The solution was injected at 4 °C into 1.2 mL of phosphate buffer (50 mM, pH* 9.0) containing 100 mM KCN and a 3.0-fold molar excess of bovine hemin. The pH of the solution was adjusted by addition of 200 μL of 300 mM MOPS buffer to a final pH* of 5.7.

The samples of reconstituted wild-type and H64F mutant Mb obtained at different refolding times were concentrated, and the CO complexes were prepared as described above in CO-saturated phosphate buffer (50 mM, pH* 5.6) in D_2O. The protected amide protons were identified by recording ^{1}H-^{15}N HSQC spectra. All cross-peak intensities were measured using NMRView. Each spectrum was calibrated by using the average of the signal volumes of the methyl proton signals of V68, L29, and V17 at 0.0 to −2.5 ppm in 1D proton spectra. The intensity for a given cross-peak at each time point was normalized with respect to the intensity of the same cross-peak at the final time point (6 s for H64F; 8 s for wild-type), representing the completed folding reaction.

Hydrogen Exchange Trapping Experiments on the Equilibrium Intermediate. Hydrogen exchange trapping experiments were performed as previously described (*4*). Exchange-out of amide protons in apoMb after transfer into D_2O at pH* 3.6 was quenched after a period of 5 min by the addition of heme and CO as described above, and the pH* was adjusted to a final value of 5.8. The extent of exchange for WT and H64F was monitored by observation of the ^{15}N-^{1}H HSQC spectrum.

RESULTS

Characterization of the Folded and Unfolded States of H64F ApoMb. The far-UV CD spectrum of H64F apoMb is very similar to that of the wild-type protein both in the urea and in the acid-denatured states (Figure 1A) and at neutral pH (Figure 1B). At neutral pH, the ellipticities at 222 nm are −18 000 and −15 800 deg cm^2 dmol^{-1} for the H64F and wild-type proteins, respectively, suggesting a small increase in the helicity of the apoprotein as a result of the mutation. Figure 1A shows that while urea largely abolishes helical structure in both the wild-type and H64F proteins, the unfolded states at low pH clearly contain some residual helical structure. A slightly greater propensity for helical structure (∼17% helix content) is observed for the acid-unfolded state of the H64F mutant protein.

The fluorescence emission maximum (data not shown) for H64F apoMb is slightly blue-shifted relative to wild-type;

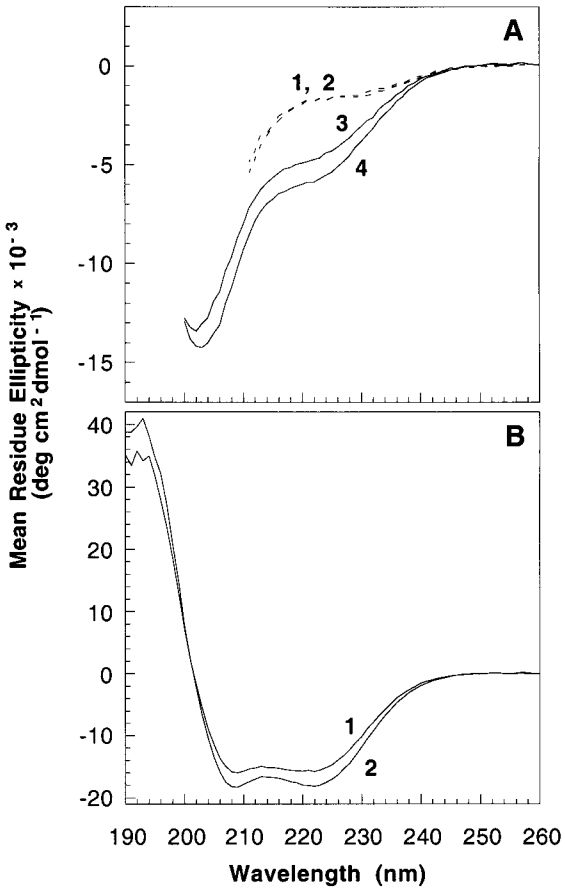

FIGURE 1: (A) CD spectra of unfolded wild-type and H64F apoMb (1, 2) in 5.8 M urea and 10 mM sodium acetate, pH 6.02; (3) wild-type apoMb in 10 mM sodium acetate, pH 2.08; (4) H64F mutant protein in 10 mM sodium acetate, pH 2.04. (B) CD spectra of native (1) wild-type and (2) H64F mutant apoMb in 10 mM sodium acetate, pH 6.05. Temperature was 25.0 °C.

this is usually characteristic of reduced solvent exposure of the tryptophan side chains. However, the differences in both the CD and fluorescence spectra between the mutant and wild-type apomyoglobin are quite small, indicating that the overall fold of the molecule in the native state is very similar.

Despite the significant change in the nature of the side chain at position 64, H64F mutant apoMb readily binds heme to form the holoprotein. Almost complete backbone ^{15}N, H^N, ^{13}C$^\alpha$, and ^{13}C$^\beta$ resonance assignments were made for the CO complex of the H64F mutant as a necessary preliminary to the quench-flow hydrogen exchange NMR experiments (see below). The ^{1}H-^{15}N HSQC spectrum of the H64F mutant protein (Figure 2) is very similar in all respects to that of the wild-type protein (*22*). As a result, assignments could be readily made using only 3D HNCA and CBCA(CO)NH triple resonance spectra. Resonance assignments have been deposited in the BioMagResBank (accession no. 4695).

Equilibrium Unfolding Experiments. To compare the stability of the native and intermediate forms of the wild-type and H64F apoMb, denaturation by acid and urea was monitored by both CD and fluorescence. Acid-induced unfolding of wild-type apoMb proceeds by a three-state process involving at least one highly populated intermediate (*3*, *4*, *23*, *24*). The acid denaturation curves of the wild-type and H64F mutant proteins were monitored by the change in ellipticity at 222 nm in the CD spectrum, by the change in

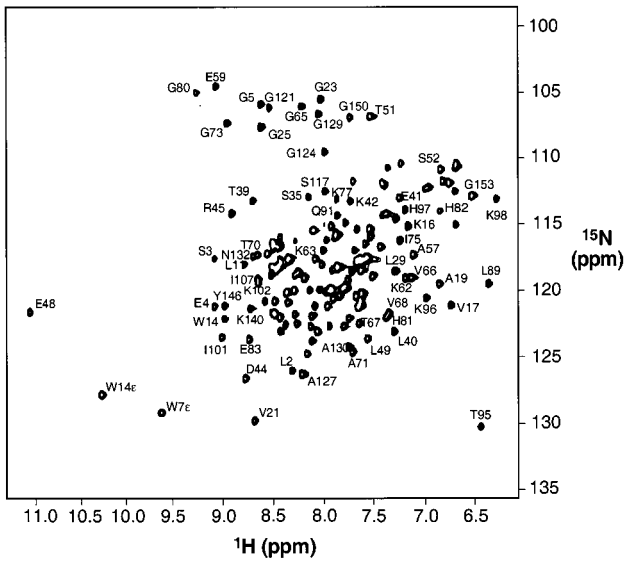

FIGURE 2: 500 MHz heteronuclear single quantum correlated NMR spectrum of ^{15}N-labeled recombinant H64F MbCO in 50 mM phosphate buffer at pH 5.7, 35 °C. Assignments for backbone resonances made using triple resonance experiments are shown in the less crowded spectral regions.

the intensity of fluorescence emission at 320 nm, and by the change in the tryptophan fluorescence anisotropy as a function of pH. Fluorescence anisotropy is a particularly convenient probe because it is highly sensitive to the presence of the apoMb intermediate state and because it is insensitive to small differences in concentration between different samples. The fluorescence anisotropy of wild-type and H64F mutant apoMb as a function of pH is shown in Figure 3A. The unfolding curves are reversible and show the presence of a compact intermediate. It is clear that both the native folded form and the intermediate of the H64F mutant are more stable against acid denaturation than is the wild-type protein. The midpoint of the N → I transition is at pH 4.45 for the wild-type protein, and at pH 3.99 for H64F. The midpoint for the I → U transition is at pH 3.11 for the wild-type and at pH 2.92 for the mutant. Measurements of the fluorescence emission intensity as a function of pH reveal the characteristic maximum associated with the intermediate state near pH 4.0 for wild-type and near pH 3.5 for the H64F mutant (Figure 3B). Formation of the intermediate at acid pH is also observed in CD spectra; the ellipticity at 222 nm is more negative for the intermediate formed by the H64F mutant, indicating a greater helical content than for the wild-type intermediate (data not shown). The fluorescence anisotropy of the wild-type and H64F apomyoglobins as a function of urea concentration is shown in Figure 3C. Once again, the mutant shows a significantly greater stability, with the midpoint of the cooperative transition at a urea concentration of 4.4 M, compared to 3.4 M for the wild-type protein. In addition, the slope of the transition appears slightly steeper for the mutant, indicating greater cooperativity. Fluorescence emission and CD measurements give similar results, and are in agreement with published fluorescence data for H64F (*10*). The urea unfolding data were analyzed using the method of Santoro and Bolen (*25*), yielding ΔG values of −3.9 and −6.7 kcal·mol^{-1} for the wild-type and mutant proteins, respectively.

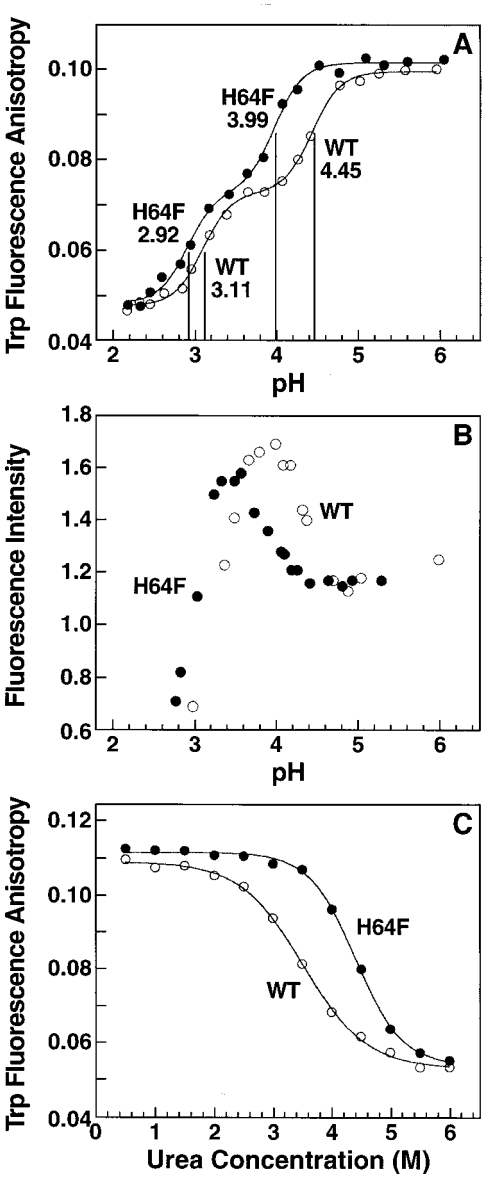

FIGURE 3: (A) Acid-induced unfolding of both wild-type and H64F mutant apoMb in 10 mM acetate buffer monitored by fluorescence anisotropy. The excitation and emission wavelengths were 280 and 336 nm, respectively. H64F apoMb shows a decrease in the pH midpoint of the transition from native (N) to intermediate (I) as well as from intermediate (I) to unfolded (U) states, indicating that both native and intermediate states of the mutant are stabilized relative to the wild-type. Data were fitted according to a model based on a linear combination of Henderson−Hasselbalch equations. For simplicity, it has been assumed that each of the two main phase transitions is driven by the collective protonation/deprotonation of a number of residues. The apparent pK_a values for the transitions of wild-type and H64F apoMb are indicated on the figure. (B) Fluorescence intensity as a function of pH for wild-type and H64F mutant apomyoglobin. (C) Urea-induced unfolding of wild-type and H64F mutant apoMb. Unfolding was monitored by fluorescence anisotropy at pH 6. The excitation and emission wavelengths were 278 and 320 nm, respectively. Data were fitted to a simple two-state model (*35*).

Both the acid unfolding and urea unfolding data clearly demonstrate that the replacement of the distal histidine in the heme pocket affects the relative stability of both native and intermediate states; compared to the wild-type apoMb, the native and intermediate states of the H64F mutant are significantly more stable.

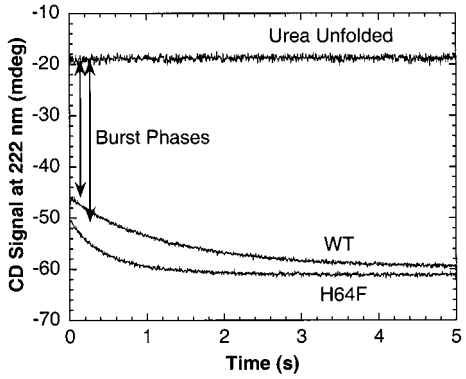

FIGURE 4: Folding kinetics of wild-type and H64F apoMb followed by monitoring ellipticity change. The experiments were carried out with rapid dilution of each protein solution from 6 to 1 M urea in 10 mM sodium acetate at 4 °C. The kinetic curves were exponentially fitted, giving first-order rate constants of 0.78 and 1.91 s^{-1} for wild-type and H64F mutant apoMb, respectively.

Refolding of ApoMb. The refolding kinetics of both wild-type and H64F mutant apoMb were monitored by Trp fluorescence and CD after stopped-flow mixing. The change in ellipticity at 222 nm following refolding of apoMb from a 6 M urea solution to a 1 M urea solution is shown for wild-type and H64F in Figure 4. Two major differences in the behavior of the two proteins are immediately apparent. The amplitude of the burst phase, where the ellipticity increases within the dead time of the stopped-flow apparatus, is substantially increased for H64F to 75% of the total ellipticity change, compared to 66% for the wild-type protein. Also, it is clear that the slower phase leading to fully folded protein is significantly faster for H64F. Exponential fitting of these two kinetic curves gives a first-order rate constant of 0.78 ± 0.06 and 1.91 ± 0.06 s^{-1} for wild-type and H64F mutant, respectively.

Quench-Flow Hydrogen-Exchange Pulse Labeling Experiments. The stopped-flow experiments show that the mutant H64F apoMb undergoes faster overall folding and has a larger kinetic burst phase amplitude than the wild-type apoMb. To characterize the kinetic intermediate and folding pathway of this mutant, we carried out hydrogen-exchange pulse labeling using a rapid quench-flow mixing procedure. Quench-flow samples were analyzed by NMR, which allows the locations of the protected amide protons to be determined. Analysis was also performed by electrospray mass spectrometry (data not shown). The quench-flow mass spectrometry results show that at the shortest refolding time (6.4 ms), the mutant protein is present entirely as the intermediate. Thus, just as in the wild-type protein, H64F apomyoglobin folds via an obligatory intermediate (*7*).

The location of secondary structure that is sufficiently stable to protect amide protons from solvent exchange can be determined by examining the ^{15}N-^{1}H HSQC spectra of samples of MbCO reconstituted from quench-flow samples obtained at various refolding times. The experiment depends on the availability of slowly exchanging amide proton probes in the holoprotein; the exchange rates and protection factors of such amides have been published (*26*). The proton occupancy for individual amide protons was obtained from the normalized intensity of the ^{1}H-^{15}N cross-peaks of each amide proton probe at different refolding times. Protection of an amide at a given refolding time implies that the residue involved participates in hydrogen-bonded helical structure in the partially folded species formed at that time.

Amide protons of about 90 residues are observable at the earliest times after transfer to D_2O solution (*26*). Of these, 59 have protection factors $\geq 10^4$, which appears to represent the lower limit of protection factor before the signal in the quench-flow experiment is too attenuated by exchange from the native state of the holoprotein. As well, there is a subset of amides which may be well protected in the holoprotein, in the presence of heme, but which are not sufficiently well protected in the folded apoprotein for signal to survive through the workup of the experiment. Hence, the total number of useful amide proton probes is 47, present primarily in the A, B, E, G, and H helices. Due to a lack of probes, the folding behavior of other parts of the protein, most notably the D and F helices, cannot be studied by this method.

The 2D ^{1}H-^{15}N HSQC spectra of the wild-type and mutant proteins after 6 ms and 6 s folding time are shown in Figure 5. It is clear that the same amide protons are protected once the two proteins are fully folded (after 6 s). However, the subset of amides that are protected in the earliest folding events differs. In the wild-type protein, amides in the A, G, and H helices and in the N-terminal part of the B helix are protected in the earliest folding events. For H64F, the protection of amides in these four helices remains largely the same, but a number of the amides in the E helix are also protected after 6 ms of folding.

This is further illustrated by a plot of proton occupancy as a function of refolding time (Figure 6). For protons in the B, C, and G helices, the refolding curves are very similar for the wild-type and H64F mutant. Parts of the A and H helices appear to show somewhat slower folding, while the majority of the E helix folds significantly faster in the mutant. The behavior of the amide proton probes in wild-type and H64F spectra is summarized in Table 1.

Characterization of the Equilibrium Intermediate of the H64F Mutant. The equilibrium unfolding data (Figure 3) show that the H64F mutant forms an intermediate during acid unfolding. This intermediate appears to form at lower pH and to be more stable than that formed by the wild-type apoMb. Amide proton exchange trapping experiments were carried out in order to determine whether the equilibrium molten globule resembles the intermediate formed during kinetic refolding of H64F. 2D ^{1}H-^{15}N HSQC spectra of the reconstituted MbCO complex after 5 min incubation of the apoprotein in D_2O at pH* 3.6 are shown in Figure 7 for both the mutant and wild-type proteins. Under these conditions, the partly folded intermediate is well populated for both proteins (see Figure 3A,B). Substantial differences are observed in the cross-peak intensities for the residues located in the E helix. In the case of the wild-type apoMb, cross-peaks of residues located in the E helix are very weak, since their amide protons are only weakly protected. For the H64F mutant, however, the resonances of E helix residues are as intense as those from the A, G, and H helices, showing that the E helix is folded and relatively stable against amide proton exchange in the equilibrium intermediate. Thus, just as for the wild-type protein (*4*, *5*), the equilibrium and kinetic intermediates of the H64F mutant appear to be similar in structure.

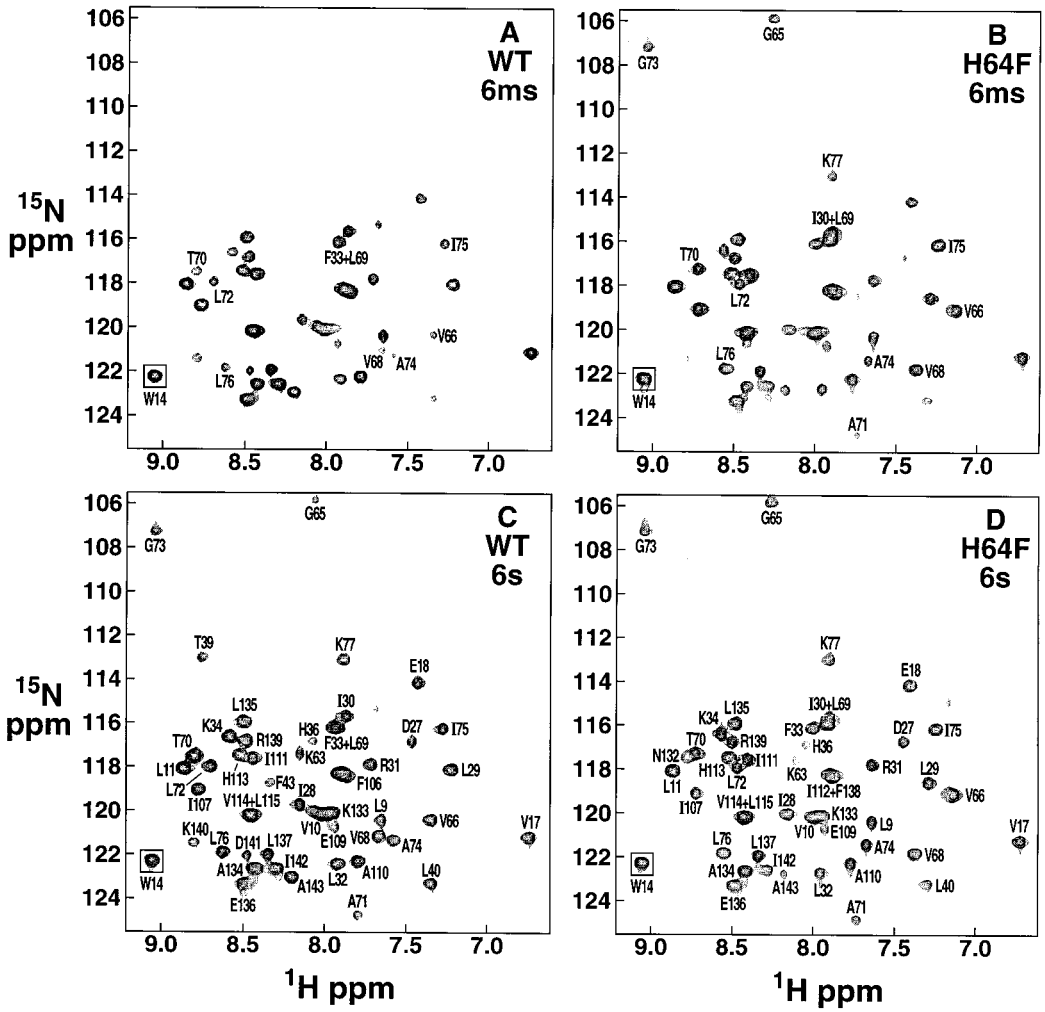

FIGURE 5: 500 MHz heteronuclear single quantum correlated NMR spectra of (A, C) wild-type and (B, D) H64F mutant apoMb recorded at 6 ms (A, B) and 6 s (C, D) after initiation of refolding. Only the amide protons from residues located in the E helix have been labeled in panels A and B. The amide proton cross-peak for Trp14 (boxed) was used to normalize the intensities of the four spectra.

DISCUSSION

Effect of the H64F Mutation on the Stability of Native ApoMb. In agreement with previous observations (*10*), the His to Phe mutation at position 64, which is located in the second turn of the E helix, promotes an overall stabilization of the native state structure relative to wild-type apoMb. In addition, there appears to be a slight increase in the helicity of the native apoprotein (Figure 1).

The mutant protein is more stable to denaturation by both acid and urea (Figure 3). The pK_a for the transition from native (N) to intermediate (I) for the mutant is 3.99, compared to 4.45 for the wild-type protein. The N $\rightarrow$ I transition is driven largely by protonation of His24 (*27*), which is distant from the site of the mutation at position 64. The lower N $\rightarrow$ I pK_a observed for the H64F mutant must then be due to a greater thermodynamic stability of the folded protein. The secondary and tertiary structure of apomyoglobin is very similar to that of the holoprotein, except that the F helix region is dynamically disordered (*1, 28*). In the wild-type holoprotein, His64 is located in a hydrophobic pocket formed by Leu29, Phe43, Phe46, Leu61, and Val68. Its pK_a is significantly lowered [pK_a 4.4−4.8 (*29*)] due to its hydrophobic environment and protection from solvent (*30*). The pK_a of His64 is lowered to a similar value (4.8) in the apoprotein (*27*), and it is therefore likely that the distal histidine residue is located in a similar hydrophobic environment whether the heme is present or not. The energetic cost of desolvation of the buried His64 side chain is expected to result in destabilization of the native apoprotein relative to unfolded states in which the histidine is both protonated and solvent-exposed (*31*). Based on the measured pK_a of His64, the extent of destabilization of the native apomyoglobin is estimated to be ca. 2.3 kcal·mol^{-1}, in good agreement with the $\Delta\Delta G$ for mutation of His64 to Phe (2.8 kcal·mol^{-1}) estimated from the urea denaturation curves of Figure 3. Not surprisingly, substitution of phenylalanine or other apolar residues (*10*) at position 64 results in significant stabilization of the native folded state. His64 is clearly required for function, to enhance the O_2 affinity through hydrogen bonding, but is conserved at the expense of globin stability (*10*). It is notable that the H64F substitution does not stabilize structure in the F helix region of the apoprotein; the F helix resonances are missing from the HSQC spectrum of the apo form of H64F myoglobin (data not shown), just as they are for the wild-type protein (*1*).

In contrast to the N132G,E136G double mutant, in which destabilization of the folded apomyoglobin is due in part at least to a decrease in H helix propensity (*9*), the H64F

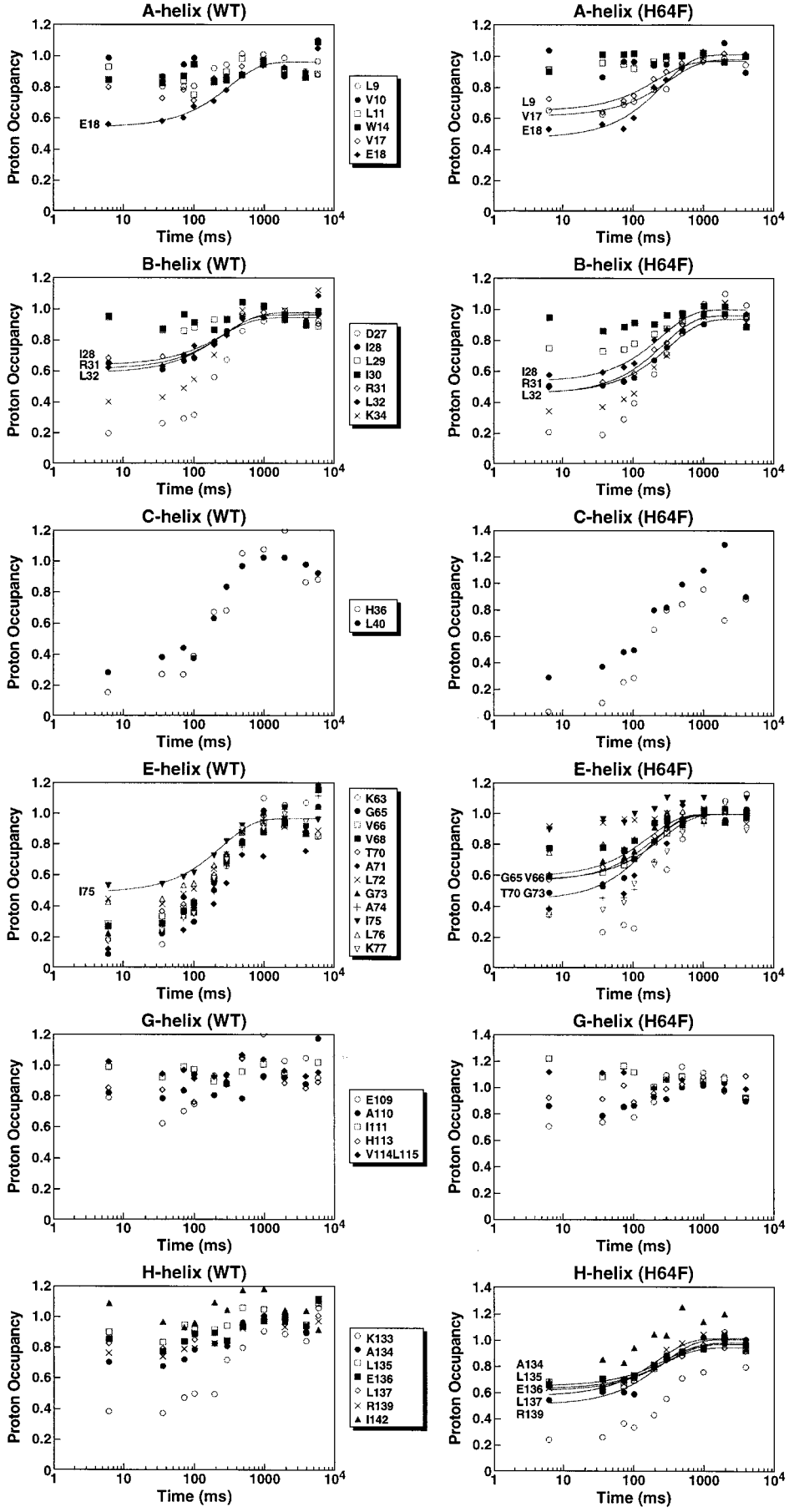

FIGURE 6: Time course of protection of backbone amide protons from exchange with solvent deuterons for wild-type and H64F mutant apoMb. Proton occupancies, derived from the intensities of the ^{1}H-^{15}N cross-peaks in the HSQC spectrum, are plotted against refolding time before the labeling pulse.

Table 1: Comparison of Behavior of Amide Proton Probes in Quench-Flow Hydrogen Exchange Experiments in Wild-Type and H64F Apomyoglobin

helix	residue	WT	H64F
A	Leu 9	F[a]	biphasic
	Val 10	F	F
	Leu 11	F	F
	Trp 14	F	F
	Val 17	F	biphasic
	Glu 18	biphasic	biphasic
B	Asp 27	S	S
	Ile 28	biphasic	biphasic
	Leu 29	F	F
	Ile 30	F	(o/l Leu 69)[b]
	Arg 31	biphasic	biphasic
	Leu 32	biphasic	biphasic
	Phe 33	(o/l Leu 69)[b]	biphasic
	Lys 34	S	S
C	His 36	S	S
	Leu 40	S	S
E	Lys 63	S	S
	Gly 65	S	biphasic
	Val 66	S	biphasic
	Val 68	S	F
	Leu 69	(o/l Phe 33)[b]	(o/l Ile 30)[b]
	Thr 70	S	biphasic
	Ala 71	S	biphasic
	Leu 72	S	F
	Gly 73	S	biphasic
	Ala 74	S	S
	Ile 75	biphasic	F
	Leu 76	S	F
	Lys 77	S	S
G	Glu 109	F	F
	Ala 110	F	F
	Ile 111	F	F
	His 113	F	F
	Val 114	F (o/l Leu 115)[c]	F (o/l Leu 115)[c]
	Leu 115	F (o/l Val 114)[c]	F (o/l Val 114)[c]
H	Asn 132	−	S
	Lys 133	S	S
	Ala 134	F	biphasic
	Leu 135	F	biphasic
	Glu 136	F	biphasic
	Leu 137	F	biphasic
	Arg 139	F	biphasic
	Ile 142	F	biphasic
	Ala 143	F	F

[a] F = amides that are fully protected at the earliest folding times (Figure 6); S = amides that are protected on a slower time scale; biphasic = amides that show biphasic behavior, with significant amplitudes of protection both in the initial refolding times and in the slower phase (see Figure 6). [b] Overlap between the cross-peak for this amide and the indicated amide in the ^{15}N HSQC spectrum. [c] Val 114 and Leu 115 are overlapped, but the cross-peak is of two-proton intensity in all spectra, indicating that both of these protons are protected on the F time scale.

mutation is unlikely to result in significant changes in intrinsic helical stability. The intrinsic helical propensities of the myoglobin sequence have been evaluated for the acid-unfolded state and for peptide fragments of the protein (*24*, *32*, *33*). The intrinsic helicity of the E helix region is very small and, given the similar helical preferences of deprotonated His and Phe (*34*), it is unlikely that the H64F mutation will significantly increase the tendency of the E helix to spontaneously adopt folded secondary structure.

Effect of the H64F Mutation on the Stability of the pH 4 Intermediate. Like the N → I transition, the transition from I to the unfolded form (U) occurs with a lower pK_a for the mutant (2.92 compared to 3.11), implying that the intermediate, too, is more stable to acid unfolding in the mutant protein than in the wild-type. The pH 4 intermediate also contains a higher content of helical secondary structure as evidenced by CD. Equilibrium amide proton exchange experiments for the I state (Figure 7) show that the E helix in the equilibrium intermediate is more stable to exchange in the mutant than in the wild-type protein.

It is clear from a comparison of the amplitudes of the burst phases in the stopped-flow CD (Figure 4), that the kinetic folding intermediate contains more helical secondary structure in the mutant than in the wild-type protein. The quench-flow NMR experiments (Figures 5 and 6) show that the amide protons of the E helix are significantly more protected in the kinetic intermediate formed by H64F than in that of the wild-type protein. Thus, the increase in helical structure observed in the stopped-flow CD burst phase is most likely due to the stabilization of helical secondary structure in the E helix.

Comparison of Folding Pathways of Wild-Type and H64F Apomyoglobin. Quench-flow hydrogen exchange NMR studies of wild-type apomyoglobin have been reported previously (*5*). These experiments were performed using two-dimensional homonuclear ^{1}H-^{1}H NOESY spectra to detect the protected amides, since ^{15}N-labeled protein was not available at that time. In the present work, ^{15}N-labeled protein was used, and exchange protection was monitored using two-dimensional HSQC spectra. The results of the new experiments (Figure 6) are in good agreement with those obtained previously (*5*). The A, G, and H helices and a part of the B helix are stabilized in the burst phase intermediate, while the helical structure in the remainder of the B helix and in the C and E helices is stabilized during slower folding events. The improved precision of the new experiments and the availability of additional amide proton probes reveal some additional features that were not clear from the earlier homonuclear NMR experiments. Some of the amides in the A (E18), B (I28, R31, L32), E (L72, I75, L76), and H (K133) helices are observed to be protected in a biphasic process, where significant protection occurs in the burst phase but complete protection is only attained during the slow folding steps. Such behavior can be attributed to a number of factors, including rapid amide proton exchange from the burst phase intermediate, structural heterogeneity of the intermediate state, and insufficient strength of the labeling pulse. Experiments performed over a range of labeling pulse pH values and times eliminate the last possibility and indicate that the biphasic protection displayed by most of these amide protons arises from structural heterogeneity of the burst phase intermediate (C. Nishimura, H. J. Dyson, and P. E. Wright, unpublished data). The quench-flow pulse labeling data for H64F are shown in Table 1 and Figure 6, and are mapped onto the structure of myoglobin in Figure 8a. Several differences are evident in the folding pathway of the H64F mutant. The most obvious difference is in the high level of burst phase protection of several amide protons in the E helix (V68, L72, I75, and L76). These residues lie along the hydrophobic face of the E helix, forming part of the interface with helices A, G, and H in the folded myoglobin structure. In addition, the amide protons of G65, V66, T70, and G73 show biphasic protection patterns, with 50−60% occupancy

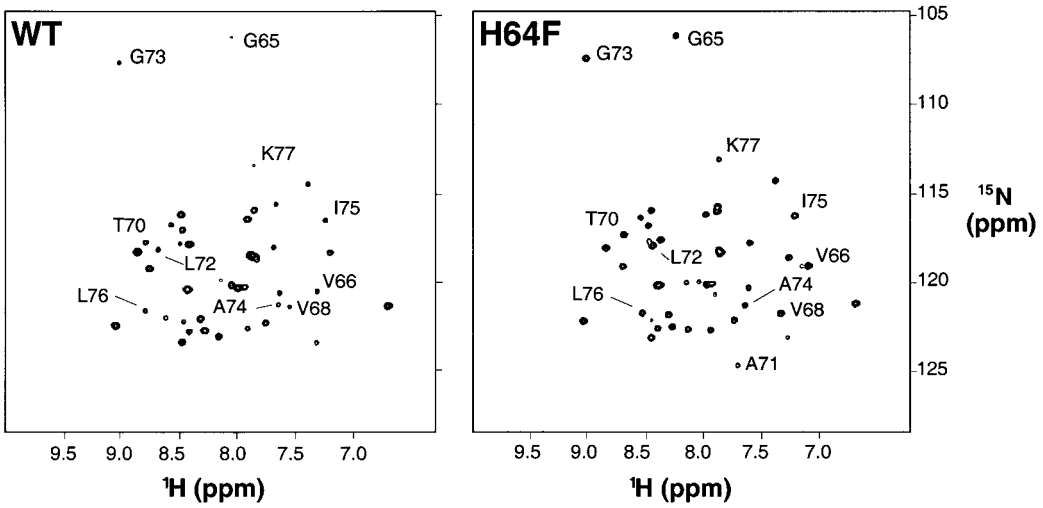

FIGURE 7: 500 MHz heteronuclear single quantum correlated NMR spectra of wild-type and H64F mutant MbCO following exchange-out of amide protons in apoMb after transfer into D_2O at pH* 3.6. The exchange was quenched after a period of 5 min by the addition of heme and CO and the pH* adjusted to a final value of 5.8.

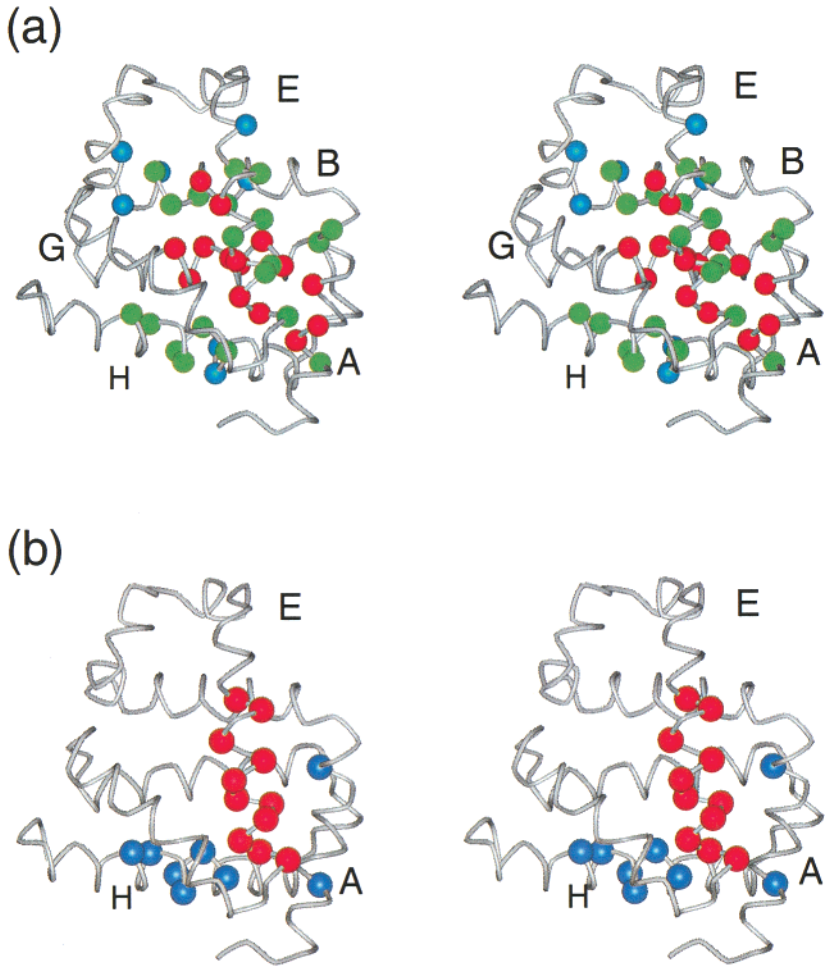

FIGURE 8: Stereoview of the backbone Cα trace of MbCO (*36*) showing: (a) the positions of the amides in H64F which are protected in the burst phase intermediate (red spheres), on the slow time scale (blue spheres), and with biphasic kinetics (green spheres); (b) amides that show changes in protection rates between wild-type and H64F apomyoglobin. Red spheres indicate residues (all of which are in the E helix) that exhibit higher burst phase proton occupancy in the H64F mutant, i.e., correspond to regions where helical structure has been stabilized in the intermediate by the mutation. Blue spheres indicate amides that display reduced proton occupancies in the burst phase intermediate formed by H64F; all are in the A and H helices and indicate a decreased population of stable helical structures in the burst phase ensemble.

in the burst phase intermediate. The amides of A71, A74, and K77 also appear to be protected in a biphasic process, but with lower burst phase occupancies. All of the observable amides in the G helix are essentially completely exchange-protected in the burst phase of H64F, as in the wild-type protein. Surprisingly, the A and H helices appear to be

slightly destabilized in the H64F intermediate. Whereas all of the observable amides in the H helix of the wild-type protein, with the sole exception of Lys133, are almost fully protected in the burst phase (Figure 6), they exhibit biphasic protection patterns during refolding of H64F. Similarly, protection of Val10 and Val17 occurs in the fast phase for wild-type apomyoglobin but occurs in a biphasic manner for H64F. The qualitative differences in folding behavior are shown mapped onto the myoglobin structure in Figure 8b. It is notable that the destabilizing effect of the mutation on the A and H helices is manifest as a biphasic folding reaction: there is a reduction in the population of molecules in the burst phase ensemble in which the A and H helices are fully stabilized. However, the stopped-flow CD experiments clearly show that formation and stabilization of the E helix does not occur in place of the A and H helices, since the H64F mutant contains significantly more helical structure in the burst phase intermediate than does the wild-type protein. The extensive regions in which biphasic protection patterns are observed suggest that there is considerable heterogeneity in the stability and location of secondary structure in the burst phase intermediate.

Role of the E Helix in ApoMb Folding. The nature of the side chain at residue 64 clearly has a major impact on both the stability of the apoprotein and on the rate and pathway of folding. In wild-type apoMb, folding commences with the formation of a compact hydrophobic core which stabilizes the A, G, and H helices and a part of the B helix. Fluctuating helical structures are formed outside this core, in the E helix, for example, but they are not sufficiently stabilized for the amide protons to be protected against exchange at the earliest refolding times. The E helix sequence has little propensity to fold spontaneously and is not found to be stabilized in helical structure either in the pH 2.3 acid unfolded state (*24*) or in peptide fragments (*33*). Likewise, the secondary structure of the E helix is not stabilized to any significant extent in the pH 4 molten globule intermediate (*24*). The replacement of a single polar amino acid, His64, by a hydrophobic residue considerably increases the stability of the native and intermediate states of apomyoglobin. In essence, the substitution of a hydrophobic side chain at position 64 alleviates the destabilizing effect of the histidine, arising from the energetic cost of desolvation and deprotonation of the imidazole group required for packing in the hydrophobic core. In contrast, a phenylalanine side chain at this position can readily become incorporated into the core and contribute favorably to its stability. As a consequence, the E helix region now plays a key role in formation and stabilization of both the kinetic folding intermediate and the equilibrium molten globule. The enhanced interactions with the core that result from the H64F mutation help to stabilize secondary structure in the E helix, albeit at the cost of some destabilization of secondary structure in the H helix (and to a lesser extent, helix A). The early incorporation of the E helix into the molten globule intermediate leads to an increased rate of folding of apomyoglobin to its native state (rate constant for folding increases from 0.78 to 1.91 s^{-1}). Thus, the present results emphasize the interplay between hydrophobic interactions and secondary structure formation in determining folding kinetics and the location and stability of secondary structure in folding intermediates. It is clear that hydrophobic interactions play a major role in stabilizing the E helix in the early folded intermediates of apomyoglobin.

Finally, the present studies of the H64F mutant, in accord with earlier experiments (*10*), reveal an inverse relationship between stability and function. Histidine 64 plays a crucial role in enhancing oxygen binding to myoglobin and in discrimination against binding of CO. The increase in stability of the native and intermediate states of apomyoglobin when this residue is changed to a phenylalanine shows that efficiency of function is achieved at the expense of both folding rate and overall stability.

ACKNOWLEDGMENT

We thank Linda Tennant and Martine Reymond for expert technical assistance, Dr. John Chung for help with NMR experiments, Dr. Maria Yamout for help with site-directed mutagenesis, and David Eliezer, Jian Yao, Vickie Tsui, Yawen Bai, and Stefan Prytulla for valuable discussions.

REFERENCES

1. Eliezer, D., and Wright, P. (1996) *J. Mol. Biol. 263*, 531−538.
2. Lecomte, J. T., Sukits, S. F., Bhattacharjya, S., and Falzone, C. J. (1999) *Protein Sci. 8*, 1484−1491.
3. Griko, Y. V., Privalov, P. L., Venyaminov, S. Y., and Kutyshenko, V. P. (1988) *J. Mol. Biol. 202*, 127−138.
4. Hughson, F. M., Wright, P. E., and Baldwin, R. L. (1990) *Science 249*, 1544−1548.
5. Jennings, P. A., and Wright, P. E. (1993) *Science 262*, 892−896.
6. Jamin, M., and Baldwin, R. L. (1998) *J. Mol. Biol. 276*, 491−504.
7. Tsui, V., Garcia, C., Cavagnero, S., Siuzdak, G., Dyson, H. J., and Wright, P. E. (1999) *Protein Sci. 8*, 45−49.
8. Matouschek, A., Kellis, J. T., Jr., Serrano, L., and Fersht, A. R. (1989) *Nature 340*, 122−126.
9. Cavagnero, S., Dyson, H. J., and Wright, P. E. (1999) *J. Mol. Biol. 285*, 269−282.
10. Hargrove, M. S., Krzywda, S., Wilkinson, A. J., Dou, Y., Ikeda-Saito, M., and Olson, J. S. (1994) *Biochemistry 33*, 11767−11775.
11. Rohlfs, R. J., Mathews, A. J., Carver, T. E., Olson, J. S., Springer, B. A., Egeberg, K. D., and Sligar, S. G. (1990) *J. Biol. Chem. 265*, 3168−3176.
12. Quillin, M. L., Arduini, R. M., Olson, J. S., and Phillips, G. N., Jr. (1993) *J. Mol. Biol. 234*, 140−155.
13. Brantley, R. E., Jr., Smerdon, S. J., Wilinson, A. J., Singleton, E. W., and Olson, J. S. (1993) *J. Biol. Chem. 268*, 6995−7010.
14. Jennings, P. A., Stone, M. J., and Wright, P. E. (1995) *J. Biomol. NMR 6*, 271−276.
15. Norwood, T. J., Boyd, J., Soffe, N., and Campbell, I. D. (1990) *J. Am. Chem. Soc. 112*, 9638−9640.
16. Marion, D., Ikura, M., Tschudin, R., and Bax, A. (1989) *J. Magn. Reson. 85*, 393−399.
17. Grzesiek, S., and Bax, A. (1992) *J. Magn. Reson. 96*, 432−440.
18. Grzesiek, S., and Bax, A. (1992) *J. Am. Chem. Soc. 114*, 6291−6293.
19. Johnson, B. A., and Blevins, R. A. (1994) *J. Chem. Phys. 29*, 1012−1014.
20. Roder, H., Elöve, G. A., and Englander, S. W. (1988) *Nature 335*, 700−704.
21. Udgaonkar, J. B., and Baldwin, R. L. (1988) *Nature 335*, 694−699.
22. Thériault, Y., Pochapsky, T. C., Dalvit, C., Chiu, M. L., Sligar, S. G., and Wright, P. E. (1994) *J. Biomol. NMR 4*, 491−504.
23. Barrick, D., and Baldwin, R. L. (1993) *Biochemistry 32*, 3790−3796.

24. Eliezer, D., Yao, J., Dyson, H. J., and Wright, P. E. (1998) *Nat. Struct. Biol. 5*, 148−155.
25. Santoro, M. M., and Bolen, D. W. (1988) *Biochemistry 27*, 8063−8068.
26. Cavagnero, S., Thériault, Y., Narula, S. S., Dyson, H. J., and Wright, P. E. (2000) *Protein Sci. 9*, 186−193.
27. Geierstanger, B., Jamin, M., Volkman, B. F., and Baldwin, R. L. (1998) *Biochemistry 37*, 4254−4265.
28. Lecomte, J. T. J., Kao, Y. H., and Cocco, M. J. (1996) *Proteins: Struct., Funct., Genet. 25*, 267−285.
29. Morikis, D., Champion, P. M., Springer, B. A., and Sligar, S. G. (1989) *Biochemistry 28*, 4791−4800.
30. Bashford, D., Case, D. A., Dalvit, C., Tennant, L., and Wright, P. E. (1993) *Biochemistry 32*, 8045−8056.
31. Yang, A.-S., and Honig, B. (1994) *J. Mol. Biol. 237*, 602−614.
32. Waltho, J. P., Feher, V. A., Merutka, G., Dyson, H. J., and Wright, P. E. (1993) *Biochemistry 32*, 6337−6347.
33. Reymond, M. T., Merutka, G., Dyson, H. J., and Wright, P. E. (1997) *Protein Sci. 6*, 706−716.
34. Pace, C. N., and Scholtz, J. M. (1998) *Biophys. J. 75*, 422−427.
35. Santoro, M. M., and Bolen, D. W. (1988) *Biochemistry 27*, 8063−8068.
36. Kuriyan, J., Wilz, S., Karplus, M., and Petsko, G. A. (1986) *J. Mol. Biol. 192*, 133−154.

BI0010266